ORIGINAL ARTICLE

Simulation of corrosion field measurement on reinforced concrete using BEM

M. Ihsan[1,4], S. Fonna[2], N. Islami,[3] Faizar[3], and A. K. Ariffin[4]

[1] Faculty of Engineering, Universitas Gajah Putih 24552, Takengon, Indonesia
[2] Department of Mechanical & Industrial Engineering, Universitas Syiah Kuala, Banda Aceh, Indonesia
[3] Electrical Engineering Department, National Islamic University of Indonesia, Bireun, Aceh, Indonesia
[4] Centre for Integrated Design for Advanced Mechanical Systems, Universiti Kebangsaan Malaysia Bangi, Malaysia

ABSTRACT – Reinforced concrete (RC) corrosion is a leading of structural deterioration and premature degradation for the infrasturctures, with significant affected for safety, durability and reability. Therefore, early assessment of RC corrosion is important to prevent deterioration of the structure. The objective of this paper is to apply Boundary Element Method (BEM) for improving reinforced concrete (RC) corrosion assessment using field measurement data. In this study, the potential on whole domain of concrete structures was modeled by Laplace equation. The Laplace equation was solved by BEM, hence the potential on the concrete structure can be determined. The field data were measured by using half-cell potential technique and collected from an existing house in Aceh region that struck by the 2004 Sumatra tsunami. The simulation results show the use of BEM can improve the RC corrosion assessment. According to ASTM C876, the distribution of potential values on the concrete surface above the corroded area were in range -200 mV to -350 mV that indicated active corrosion was occurred. It can be inferred, the method can improve the field measurement data since it has capability to predict the corrosion profiles of reinforcing steel in more precise.

INTRODUCTION

Reinforced concrete (RC) is the most widely used as a main material for structure construction [1]. Since of reduction of quality and aging of concrete structures and the intensity of the increased traffic and loads are some of the major problems faced by the civil engineers or researchers today. Therefore, early investigation of concrete structure reduction become important. Many researchers has been investigate the several causes of the problems. Early deterioration of concrete due to several factors such as aggressive environments, and poor quality construction has occurred in many reinforcing steel structures [2,3]. The result also inferred that corrosion is also one of the main causes of the concrete reduction quality and it can lead to premature failure [4]. Therefore, performing corrosion assessment periodically for the maintenance of a concrete structure is important [5,6]. It can reveal the corrosion damage process of reinforced concrete (RC) in the structures being investigated and controlled.

Recent year, more attention has been given by some researchers for corrosion assessment of reinforced concrete. Field measurement is one of the conventional strategies for reinforcing steel corrosion assessment. Some techniques are introduced for field corrosion assessment such as half-cell potential technique [7]. The method influence by the environment factors [8] and needs electrical access to the steel. High impedance voltmeter and a reference electrode should be connected, in contact with the steel and surface of reinforced concrete respectively [9–11]. The method is difficult to be done in many cases such as the part of RC structures those have limited access such as corrosion control in traffic bridge [12,13] and marine infrastructures [14]. The method will cost a large amount of resurches and time consuming [15]. Concrete condition factors such as the concrete cover thickness [16,17] and concrete porosity [18] also influence the measurement results, because the measurements are only done on the surface of the concrete. The measurement result also influenced by certain environment [19] and current condition of RC structues. The methods only report the corrosion risk level and the results are not able to give a direct assessment of the reinforced concrete corrosion. Therefore, due to the several experimental difficulties, it can be a major challenge for the field assessment that might lead to misleading prediction of RC corrosion. A reliable investigation method is required for decrease the limitation of field measurement. Some researchers have introduced computational approach for solving the problem. The most widely used numerical techniques for solving the experimental difficulties analysis and field assessment that migh lead to misleading such as Finite element method (FEM) (e.g. [20,21]) and Boundary element method (BEM) (e.g [22,23]. However, the method (FEM) requires the discretization of the whole domain and can be an extremely tedious and time-consuming process. Whereas, reinforced concrete corrosion asessment only needs the potential data on the concrete surface. Thus, BEM consider able to reduce misleading prediction of field measurement. In this research, BEM were apply to reduce the field measurement effort for corrosion assesment. The significance of this research is able to reduce the field measurement data value collection and predict the corrosion occuring in reinforcing steel. Furthermore, the validation of

corrosion assessed by BEM will be validate with actual observation on the assesed reinforced concrete column. The assesed reinforcing steel building which was affected by 2004 tsunami Sumatra.

METHODS AND MATERIALS

Half-cell Potential Technique

Half-cell potential technique consists of a device comprising of a piece of metal in a solution such as copper ions in copper sulphate and silver in silver chloride. The method also one of non-destructive techniques for RC corrosion risk assessment [15], [24]. The method is considered efficient combining with numerical approach boundary element method for reliable result. In this research, some potential data from concrete surface was collected for analyzing with numerical boundary element method. The schematic of half-cell potential technique to estimate the potential on the RC surface is shown in Figure 1.
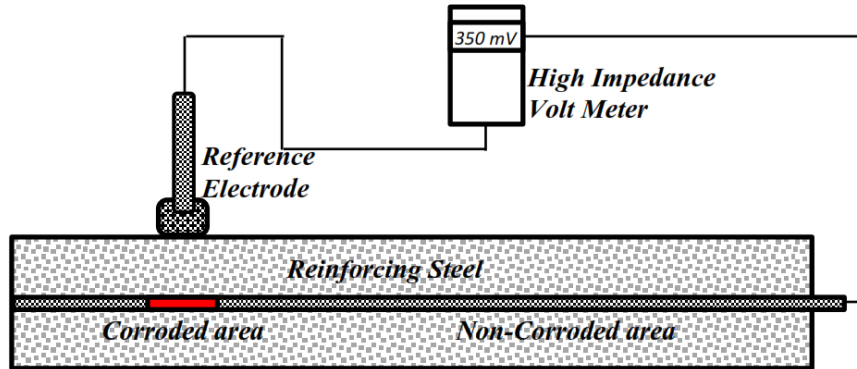

Figure 1. Schematic of half-cell potential technique

The potential measured on the concrete surface given by half-cell potential method is indication of the corrosion risk level of the steel. ASTM C876 [25] gives a way to interpret half-cell potential measurement data in the field. Table 1 describes the criteria of reinforced concrete corrosion risk. The potential measured by the half-cell potential is relatively low if the steel is in passive state, 0 to −200mV (Cu/CuSO4). Corrosion actively occurs when the potential is more negative than −350mV. The potential reading moves toward the potential value of −350mV when the passive layer is failing.

Table 1. The ASTM C876 criteria for corrosion risk of reinforced concrete

References electrode Cu/CuSO$_4$	References electrode Ag/AgCl	Corrosion Risk
≥ -200 mV	≥ -106 mV	Low (10% risk of corrosion)
-200 to -350mV	-106 to -256 mV	Intermediate corrosion risk
≤ -350 mV	≤ -256 mV	High (<90% risk of corrosion)
≤ -500 mV	≤ -406 mV	Severe corrosion

Numerical Modeling Bem of Reinforcing Steel Corrosion

The potential of the concrete domain (Ω) region can be modeled mathematically by the Laplace's equation [26]:

$$\nabla^2\phi = 0 \quad in \quad \Omega \tag{1}$$

where the density of current, denoted by i, is given by:

$$i = -\kappa\,\frac{\partial\phi}{\partial n} \tag{2}$$

where n is unit outward normal and $\partial/\partial n$ is derivative in the direction of normal. Boundary condition of the concrete domain is given in Figure 2. Boundary conditions, related with Eq. (1) are:

$$i = i_0 \quad on \quad \Gamma_1 \tag{3}$$

$$\phi = -f_a(i) \quad on \quad \Gamma_{2a} \tag{4}$$

$$\phi = -f_c(i) \quad on \quad \Gamma_{2c} \tag{5}$$

where ϕ is potential at any point, i is current density, $f_a(i)$ is the corroded polarization curves and $f_c(i)$ is non-corroded polarization curves of the steel in concrete. The minus signs on the right hand sides of Eqs. (4) and (5) are due to the fact that the potential in the electrolyte near the metal surface (ϕ) is equal to minus value of potential difference between the metal and the reference electrode [27]. It is noted that the potential (ϕ) is defined with referring to the metal and has the inverse sign of the employed usually in the corrosion science. The current density within the steels has been imposed as zero for the numerical calculations.
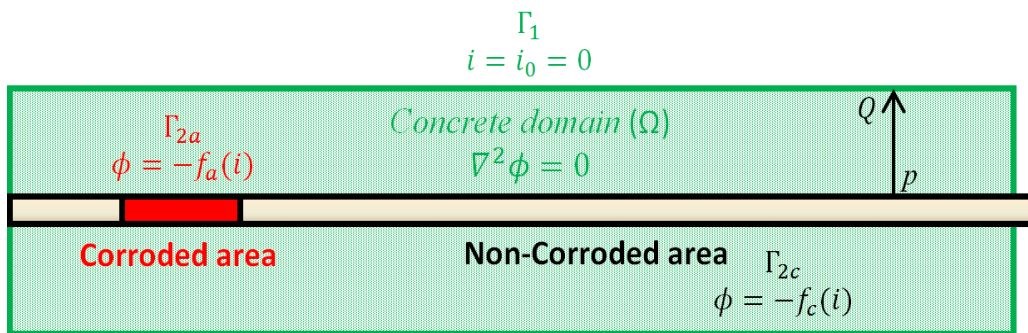

Figure 2. Boundary conditions for reinforced concrete corrosion modeling

Three dimension formulation

The differential equation representing Laplace's equation in three dimensions can be written as follows:

$$\nabla^2\phi = \frac{\partial^2\phi}{\partial x^2} + \frac{\partial^2\phi}{\partial y^2} + \frac{\partial^2\phi}{\partial z^2} = 0 \tag{6}$$

where ∇^2 is Laplacian operator and x, y and z are the Cartesian coordinates axes which is an arbitrary domain where the solution is sought. In this solution domain, assume that there is an interior point p (usually called the 'load' point) of coordinates X_p, Y_p and Z_p, and consider any point on the boundary Q (usually called the 'field' point) with coordinates x_Q, y_Q and z_Q. The use of capital letters for the coordinates indicates a fixed point, whereas the lower case coordinates indicate a variable point. The three-dimensional fundamental solution of Laplace's equation based on a concentrated potential or source at the point P can be easily verified as follows:

$$\lambda(p,Q) = \frac{1}{4\pi}\left[\frac{1}{r(p,Q)}\right] \tag{7}$$

where $r(p,Q)$ is distance between p and Q given by:

$$r(p,Q) = \sqrt{(X_p - x_Q)^2 + (Y_p - y_Q)^2 + (Z_p - z_Q)^2} \tag{8}$$

The constant $\left(\frac{1}{4\pi}\right)$ is associated with the strength of the potential at the point p but can be considered arbitrary for the present purpose.

Green's Functions

Green's functions for linear differential operators involving the Laplacian readily put to use using the second of Green's identities to solve the problem within the domain to its boundary as follows:

$$\int_\Omega \left\{ \left(\phi \nabla^2 \right) \phi^*(Q, p) - \left(\phi^* \nabla^2 (Q, p) \right) \phi \right\} \partial\Omega = \int_\Gamma \left\{ \left(\frac{\partial\phi}{\partial n} \right) \phi^*(Q, p) - \left(\frac{\partial\phi^*(Q, p)}{\partial n} \right) \phi \right\} \partial\Gamma \tag{9}$$

By applying the Laplace's equations and $-\kappa$, the solutions may be written as follows:

$$\kappa \int_\Omega \left\{ \left(\phi^* \nabla^2 (Q, p) \right) \phi \right\} \partial\Omega = \int_\Gamma \left\{ (i) \phi^*(Q, p) - \left(i^*(Q, p) \right) \phi \right\} \partial\Gamma \tag{10}$$

Eq. (10) shows the advantage of the BEM that reduction the problem dimension by one. The standard boundary element procedures derived by:

$$\kappa \left[H \right] \begin{Bmatrix} \phi_1 \\ -f(i_a) \\ -f(i_c) \end{Bmatrix} - \left[G \right] \begin{Bmatrix} i_0 \\ i_a \\ i_c \end{Bmatrix} = 0 \tag{11}$$

where the further detailed expression of $\left[H \right]$ and $\left[G \right]$ matrices are given in [28]. The known current density represented by 0. The system of non-linear algebraic equations in Eq. (11) can be solved by iterative procedures, e.g. the Newton-Raphson method and LU decomposition. Therefore, the potential ϕ and current density i on the overall surface of reinforced concrete can be determined.

RESULTS

Field Measurement Corrosion Assesment

The corrosion risk assessment of reinforced concrete has been performed on an existing house in Aceh region after six years submerged by the 2004 Sumatra tsunami in previous research. For this study, one critical column of a residential building in Peukan Bada, Aceh Besar, Province of Aceh was selected to be assessed both by potential mapping and BEM 3D corrosion simulation. The building was located 1.8 km from the shoreline and the elevation of tsunami in that region around 10 m. The building and selected column are shown in Figure 3.

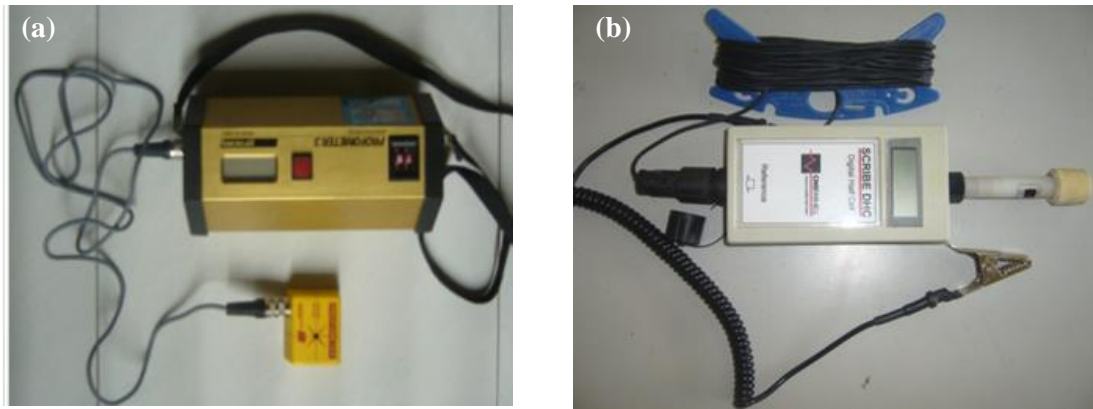**Figure 3.** Residential reinforced concrete building which was affected by 2004 tsunami Sumatra

Figure 4. The equipment of potential measurement on reinforced concrete surface: (a) Steel locator (Profometer-3) and (b) SCRIBE DHC digital half-cell meter

The location of steel in the concrete was mapped precisely using a profometer-3 as shown in Figure 4,a. Then, the corrosion potential at those mapped point was assessed by using half-cell meter as shown in Figure 4,b. The result shows that the potential corrosion distributions were varying approximately between -100 mV to -350 mV as shown in   Figure 5. The critical area was located at upper column. The potential corrosion for the upper area ranged between -200 to -350 mV. According to ASTM C876, this column was already at intermediate corrosion risk.
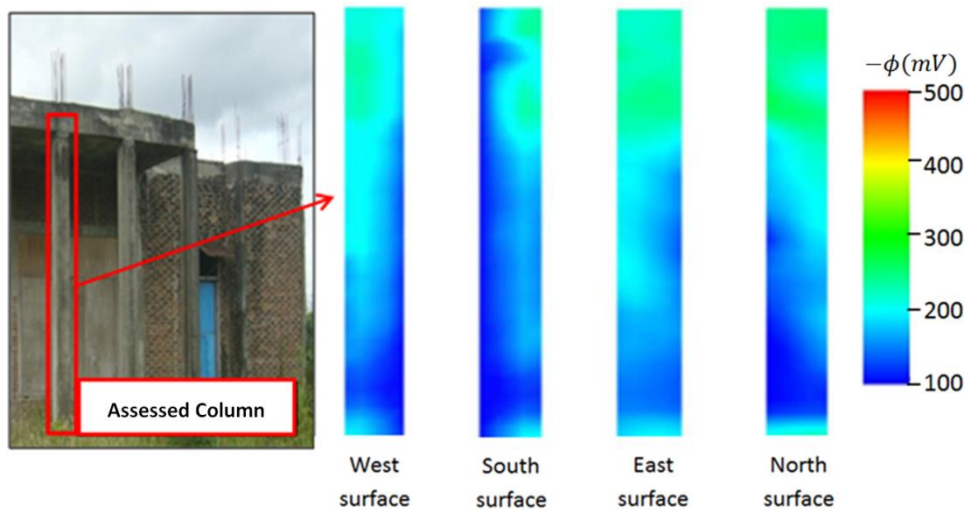

Figure 5. The potential corrosion distributions from field measurement data at the assessed column

BEM Corrosion Simulation

A model of reinforced concrete corrosion is shown in Figure 6, where the size of corroded area of the steels was 80 cm. Four rebar were embedded into concrete column. The thickness concrete cover was assumed 5 cm from the embedded rebar. For the corrosion condition for simulation, the corrosion size came from several trials-and-errors simulation in order to obtain similar potential distribution between simulation and field measurement. The conductivity of concrete (κ) was 0.007 $\Omega^{-1}m^{-1}$. The boundary conditions for the corroded and non-corroded areas on the steels were generated from linearization of the polarization curve that given in the reference [26]. The model was divided into 9589 triangle element mesh for 3D boundary element calculation.
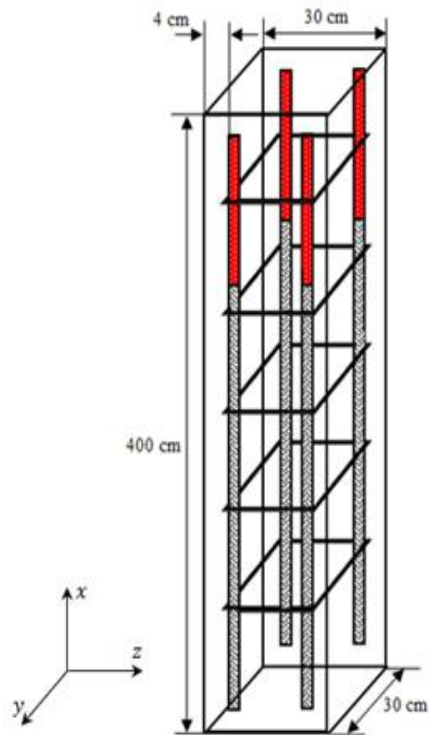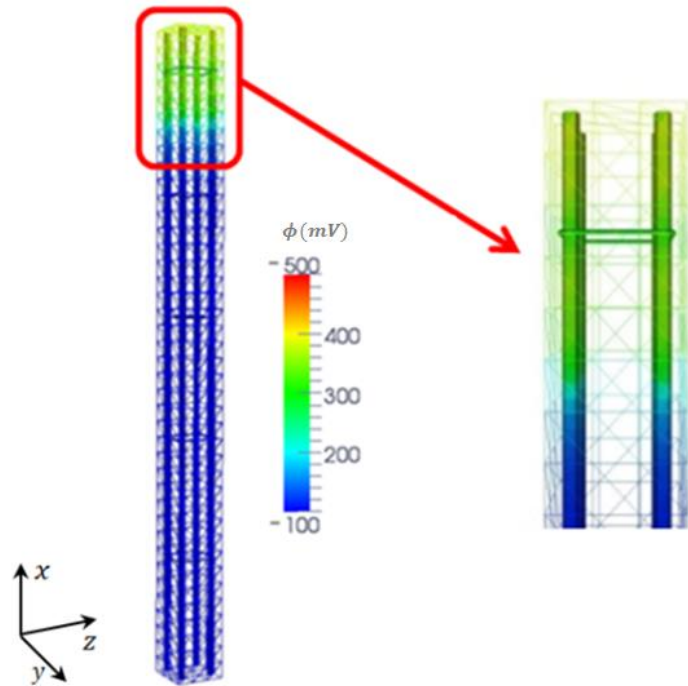
Figure 6. Model of RC Corrosion   **Figure 7.** The distribution of potential on the RC using 3D BEM

The 3D BEM was performed using the above boundary conditions. The result shows the potential distribution on whole surfaces of the steel and concrete as given in Figure 7. The potential values of upper part of the concrete surface are higher than the rest one. This indicated that the corrosion was actively occurred on the reinforcing steel of the upper part of the structure as modeled. The result also shows the potential values of corrosion were distributed in the upper part of concrete came into high risk corrosion based on Table 1.

DISCUSSION

Factor Influence Field Measurement

For comparison result, Figure 8 shows the comparison the potential distribution on the concrete surface obtained by simulation result with the field measurement result using half-cell potential mapping technique. A good agreement of the potential distribution along x-axis on concrete surface was obtained where the potential values significantly decrease above the corroded area along x-axis from 320 to 400 cm. Furthermore, the 3D BEM simulation result shows the similar corrosion risk level as given by the field measurement result. The potential values on the concrete surface above the non-corroded areas were lower than -100 mV that indicated the corrosion reaction came into low risk corrosion.

Meanwhile, the distribution of potential values on the concrete surface above the corroded area were in range -200 mV to -350 mV that indicated active corrosion was occurred. The result also shows the differences potential distribution along 0 to 200 cm of rebar (green cycle). The differences occur since current measured field condition influence. Current measured concrete condition was shown by Fig. 9. The Defect and pitting was occur on the concrete cover. Thus, it might lead a misleading of the field measurement. Therefore, many field condition factor influence the assessment result. Meanwhile, the assumed concrete conductivity of reinforced concrete influence the simulation result, the result shows a stable potential distribution along 0 to 200 cm rebar. However, the differences of potential distribution along 0 – 200 cm considered consistent with the field measurement. It's due to standar corrosion risk level in Table 1, in the 0 – 200 cm of rebar considered came to low risk corrosion.
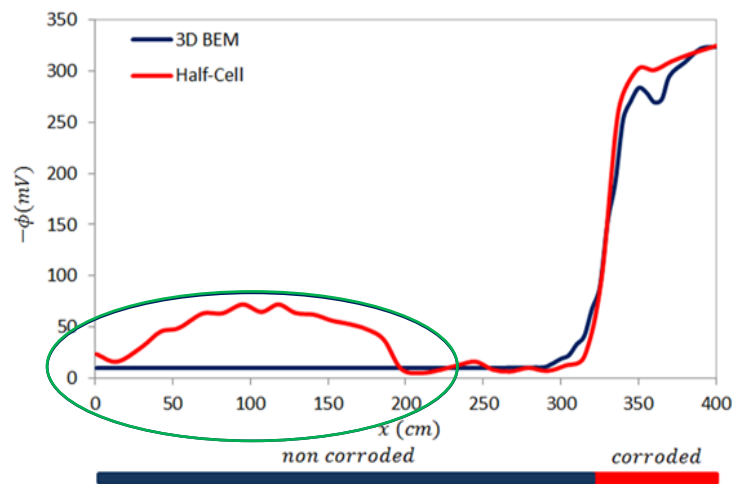
Figure 8. Potential distributions on concrete surface obtained by 3D BEM and by Half-cell measurement

In the other hand, the comparison gives an indication that the corrosion size of the actual corrosion was similar with the corrosion size in the simulation. By doing 3D BEM simulation, thus comparing the result with the assessment data, information related to the corrosion distribution might be obtained, for this case was corrosion location and size. Hence, the assessment could be improved by using 3D BEM simulation. Further analysis was obtained in the research. Actual observasion was perform to validate the field measurement and 3D BEM simulation.

Figure. 9. The current assessed concrete cover condition during field assessment

Actual Observation for Validation

The selected public buildings that were assessed have been reconstructed as shown in Figure 10. Visual observation has been conducted for the analysis of field measurement and simulation of BEM for validation. The actual observation shows that the corrosion activity has been occur on the reinforcing steel. Based on the field measurement, the enhancement of corrosion potential was occur on the bottom of rebar and high risk of corrosion activity was occur on the upper site of rebar. Meanwhile, the simulation result shows the high risk corrosion activity was occur on the upper site of reinforcing steel. Regarding those result, the bottom and upper site of assessed rebar was destroyed as shown in Figure 11.

Figure 10. The assessed concrete column was reconstructed

The actual observation shows that low risk corrosion activity was occur on the bottom site of rebar and worse corrosion has already taken place in upper site of the reinforcing steel. Figure. 11(a) shows that the high corrosion risk was occur on the upper site of concrete and Figure. 11(c) shows the low risk of corrosion on the site.
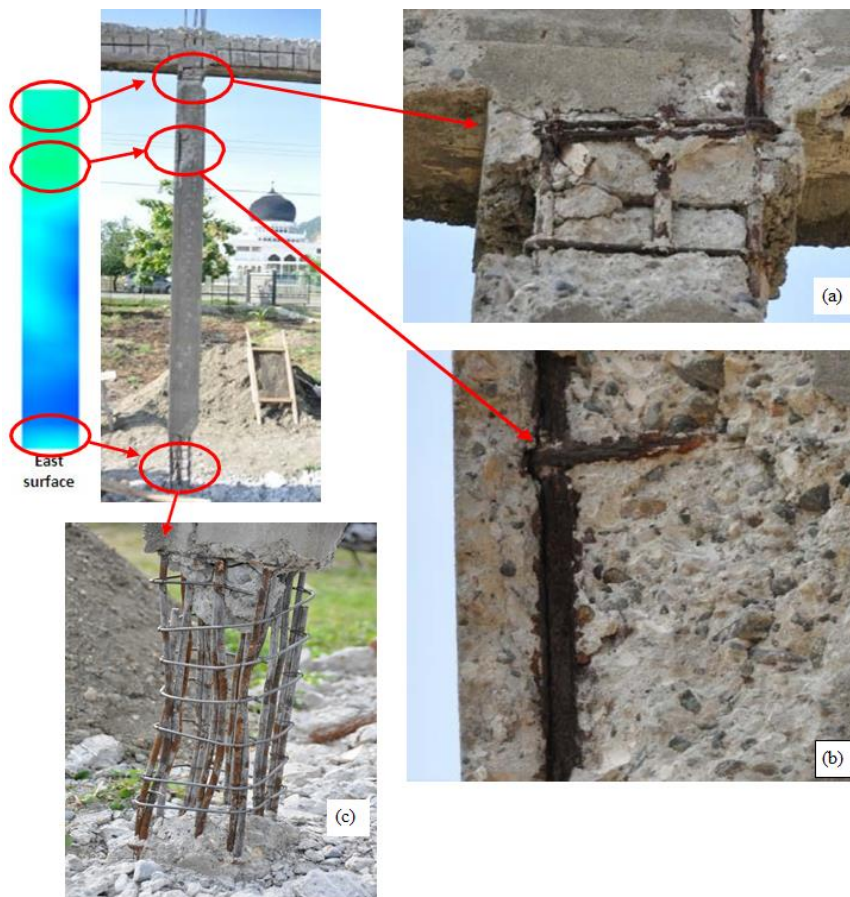

Figure. 11. Actual corrosion of rebars in the east surface of column 1 of the existing civilian house

The observation also shows that the experimental result has good accuracy in predicting the corrosion risk of reinforcing steel. Further actual for validation corrosion that already occurring in the column of the existing Tsunami building is shown in Figure 12. It can also be seen that the rebar are already corroded under the surface of the concrete, and even worse corrosion has been occur on the upper site. However, in resolving the experimental work, much time must be allocated well and many field factor must be reckoned. The current concrete condition also influence the field measurement. Hence, BEM can be an option to improve the field measurement result in order to obtain better assessment result. By using BEM, the actual corrosion condition determined by field measurement can be well predicted.

Figure. 12. The worst actual corrosion of rebar after reconstructed for actual condition prediction

CONCLUSION

The measurement field data has been collected by half-cell potential technique that show the probability of corrosion of reinforced steel of the public buildings affected by 2004 Tsunami Aceh. RC corrosion has been simulated by using 3D BEM which indicated the potential corrosion on the concrete structure was affected by corrosion profiles of the reinforcing steel. The comparison of potential distribution on the concrete surface obtained by simulation result was agreed well with the field measurement result. For such situation, the actual corrosion profile also might similar to the simulation. Therefore, RC corrosion assessment by using half-cell potential technique can be improved by employing the 3D BEM, since the corrosion profiles of reinforcing steel in more precise can be predicted. Moreover, in order to avoid the corrosion of reinforcing steel inside the concrete, several methods could be applied, i.e. cathodic protection, realkalization, and chloride removal.

REFERENCES

[1]   A. James *et al.*, "Rebar corrosion detection , protection , and rehabilitation of reinforced concrete structures in coastal environments : A review," *Constr. Build. Mater.*, vol. 224, pp. 1026–1039, 2019, doi: 10.1016/j.conbuildmat.2019.07.250.

[2]   Z. Cui, A. Alipour, and B. Shafei, "Structural performance of deteriorating reinforced concrete columns under multiple earthquake events," *Eng. Struct.*, vol. 191, pp. 460–468, Jul. 2019, doi: 10.1016/j.engstruct.2019.04.073.

[3]   X. Xing, X. Xu, J. Wang, and W. Hu, "Preparation , release and anticorrosion behavior of a multi-corrosion inhibitors-halloysite nanocomposite," *Chem. Phys. Lett.*, vol. 718, no. October 2018, pp. 69–73, 2019, doi: 10.1016/j.cplett.2019.01.033.

[4]   T. Senga Kiesse, S. Bonnet, O. Amiri, and A. Ventura, "Analysis of corrosion risk due to chloride diffusion for concrete structures in marine environment," *Mar. Struct.*, vol. 73, p. 102804, 2020, doi: https://doi.org/10.1016/j.marstruc.2020.102804.

[5]   S. Hong, H. Wiggenhauser, R. Helmerich, B. Dong, P. Dong, and F. Xing, "Long-term monitoring of reinforcement corrosion in concrete using ground penetrating radar," *Eval. Program Plann.*, 2016, doi: 10.1016/j.corsci.2016.11.003.

[6]   S. Karthick, S. Muralidharan, H. S. Lee, S. J. Kwon, and V. Saraswathy, "Reliability and long-term evaluation of GO-MnO 2 nano material as a newer corrosion monitoring sensor for reinforced concrete structures," *Cem. Concr. Compos.*, vol. 100, no. April 2017, pp. 74–84, 2019, doi: 10.1016/j.cemconcomp.2019.03.012.

[7]   S. Fonna, M. Ridha, S. Huzni, W. A. Walid, T. T. D. Mulya, and A. K. Ariffin, "Corrosion Risk of RC Buildings after Ten Years the 2004 Tsunami in Banda Aceh - Indonesia," *Procedia Eng.*, vol. 171, pp. 965–976, 2017, doi: 10.1016/j.proeng.2017.01.402.

[8]   W. Yodsudjai and T. Pattarakittam, "Factors influencing half-cell potential measurement and its relationship with corrosion level," *Meas. J. Int. Meas. Confed.*, vol. 104, pp. 159–168, 2017, doi: 10.1016/j.measurement.2017.03.027.

[9]   M. Ihsan, S. Fonna, M. Ridha, S. Huzni, and A. K. Ariffin, *The influence of anode profiles for three dimensions numerical simulation of reinforced concrete corrosion using boundary element method*, vol. 686. 2013.

[10]   G. Ebell, A. Burkert, and J. Mietz, "Detection of Reinforcement Corrosion in Reinforced Concrete Structures by Potential Mapping: Theory and Practice," *Int. J. Corros.*, vol. 2018, 2018, doi: 10.1155/2018/3027825.

[11]   D. Luo, Y. Li, J. Li, K. S. Lim, N. A. M. Nazal, and H. Ahmad, "A recent progress of steel bar corrosion diagnostic techniques in RC structures," *Sensors (Switzerland)*, vol. 19, no. 1, 2019, doi: 10.3390/s19010034.

[12]   B. A. Mazzeo, J. Baxter, J. Barton, and W. S. Guthrie, "Vertical impedance measurements of concrete bridge deck cover condition without a direct electrical connection to the reinforcing steel," *AIP Conf. Proc.*, vol. 1806, pp. 1–6, 2017, doi: 10.1063/1.4974629.

[13]   L. Bourreau *et al.*, "On-site Corrosion Monitoring - Reliability To cite this version : HAL Id : hal-01518739," 2017.

[14]   J. Alcántara, D. de la Fuente, B. Chico, J. Simancas, I. Díaz, and M. Morcillo, "Marine atmospheric corrosion of carbon steel: A review," *Materials (Basel).*, vol. 10, no. 4, 2017, doi: 10.3390/ma10040406.

[15]   A. Zaki, H. K. Chai, D. G. Aggelis, and N. Alver, "Non-destructive evaluation for corrosion monitoring in concrete: A review and capability of acoustic emission technique," *Sensors (Switzerland)*, vol. 15, no. 8, pp. 19069–19101, 2015, doi: 10.3390/s150819069.

[16]   N. M. A.- Galawi, A. A. H. Al-tameemi, and S. H. Al-jarrah, "Effect Of Age And Concrete Cover Thickness On Steel Reinforcement Corrosion At Splash Zone In Reinforced Concrete Hydraulic Structures," *Int. J. Sci. Technol. Res.*, vol. 4, no. 8, pp. 129–133, 2015.

[17]   A. Fahim, P. Ghods, O. B. Isgor, and M. D. A. Thomas, "A critical examination of corrosion rate measurement techniques applied to reinforcing steel in concrete," *Mater. Corros.*, vol. 69, no. 12, pp. 1784–1799, 2018, doi: 10.1002/maco.201810263.

[18]   M. J. Miah, M. M. H. Patoary, S. C. Paul, A. J. Babafemi, and B. Panda, "Enhancement of Mechanical Properties and Porosity of Concrete Using Steel Slag Coarse Aggregate," *Materials (Basel).*, vol. 13, no. 12, p. 2865, 2020, doi: 10.3390/ma13122865.

[19]   S. Pang, M. K. Yu, H. G. Zhu, and C. Yi, "The corrosion probability and flexural strength of an RC beam under chloride ingress considering the randomness of temperature and humidity," *Materials (Basel).*, vol. 13, no. 10, 2020, doi: 10.3390/ma13102260.

[20]   C. Hu, D. Ling, X. Ren, S. Gong, L. Wang, and Z. Huang, "An improved crack-tip element treatment for advanced FEMs," *Theor. Appl. Fract. Mech.*, vol. 108, no. April, p. 102587, 2020, doi: 10.1016/j.tafmec.2020.102587.

[21]   E. Chaparian and O. Tammisola, "An adaptive finite element method for elastoviscoplastic fluid flows," *J. Nonnewton. Fluid Mech.*, vol. 271, no. February, 2019, doi: 10.1016/j.jnnfm.2019.104148.

[22]   S. Fonna, Gunawarman, S. Huzni, and A. K. Ariffin, "Boundary element inverse analysis for rebar corrosion detection: Study on the 2004 tsunami-affected structure in Aceh," *Case Stud. Constr. Mater.*, vol. 8, pp. 292–298, Jun. 2018, doi: 10.1016/j.cscm.2018.02.008.

[23]   X. Yang, Y. Li, G. Liu, and H. Gui, "The prediction of load distribution in four-row cylindrical roller bearings under the elastohydrodynamic lubrication based on boundary element method," *Eng. Anal. Bound. Elem.*, vol. 105, no. March, pp. 242–256, 2019, doi: 10.1016/j.enganabound.2019.04.008.

[24]   O. Anterrieu, B. Giroux, E. Gloaguen, and C. Carde, "Non-destructive data assimilation as a tool to diagnose corrosion rate in reinforced concrete structures," *J. Build. Eng.*, vol. 23, no. October 2018, pp. 193–206, 2019, doi: 10.1016/j.jobe.2019.01.033.

[25]   A. ASTM, "Standard Test Method for Half-cell potentials of Uncoated Reinforcing Steel in Concrete," *ASTM Int.*, 1999.

[26]   S. Fonna, S. Huzni, A. Zaim, and A. K. Ariffin, "Simulation of cathodic protection on reinforced concrete using BEM," *J. Mech. Eng.*, vol. SI 4, no. 2, pp. 111–122, 2017.

[27]   M. Ihsan, S. Fonna, R. Kurniawan, Z. Fuadi, and A. K. Ariffin, "Computational Modelling for RC Cylindrical Column Corrosion using Axisymmetric BEM," in *Proceedings: CYBERNETICSCOM 2019 - 2019 IEEE International Conference on Cybernetics and Computational Intelligence: Towards a Smart and Human-Centered Cyber World*, 2019, doi: 10.1109/CYBERNETICSCOM.2019.8875678.

[28]   A. V. Novikov, V. S. Posvyanskii, and D. V. Posvyanskii, "An application of Green's function technique for computing well inflow without radial flow assumption," *Comput. Geosci.*, vol. 21, no. 5–6, pp. 1049–1058, 2017, doi: 10.1007/s10596-017-9684-6.